ELSEVIER

Catalysis Today 38 (1997) 181–186

CATALYSIS TODAY

A pilot plant study for selective catalytic reduction of NO by NH_3 over mordenite-type zeolite catalysts

In-Sik Nam[a,b,*], Soo Tae Choo[a,b], Dong Jun Koh[a,b], Young Gul Kim[a,b]

[a]*Research Center for Catalytic Technology, Department of Chemical Engineering, School of Environmental Engineering, Pohang University of Science and Technology (POSTECH), San 31 Hyoja Dong, Pohang 790-784, South Korea*

[b]*Environmental Catalysis Team, Research Institute of Industrial Science and Technology (RIST), San 32 Hyoja Dong, Pohang 790-300, South Korea*

Abstract

The copper-ion-exchanged synthetic mordenite and natural zeolite catalysts washcoated on a honeycomb reactor have been examined in a pilot plant for the selective catalytic reduction of NO by NH_3. The catalyst life and the cause of the catalyst deactivation were mainly investigated for the design of the commercial reactor to remove NO_x from a sintering plant at the steel mill.

Keywords: Selective catalytic reduction; Nitric oxides; Zeolite; Mordenite; Honeycomb reactor; Deactivation; Sintering plant

1. Introduction

As the regulation for the NO_x emission becomes strict, much effort has been focused on the development of more efficient NO_x removal technology. The selective catalytic reduction (SCR) of NO_x with NH_3 is the most effective and commercially proven technology to remove NO_x from stationary sources. Commercial SCR process removes 60–90% of NO_x which is a higher efficiency than that obtainable by any other commercially proven technology. Various types of catalysts including noble metals, supported metal oxides and zeolites have been proposed and examined for the reduction of NO_x with NH_3. Supported vanadium oxide catalyst, in particular, is known to be the most effective and widely used commercial SCR catalyst due to its high activity and durability to sulfur compounds [1]. Recently, transition metal ion-exchanged Y-zeolite and H-mordenite have also been reported to be effective catalysts for this reaction system [2,3].

In a previous study [4,5], it has been shown that the copper-ion-exchanged hydrogen mordenite and natural zeolite catalysts exhibited high activity at the reaction temperatures in the range of 300–400°C. The effect of SO_2 on the steady-state activity for this reaction has been also examined in a fixed-bed reactor system. It is known that sulfur compounds contained in the flue gas deactivate SCR catalysts [6]. The deactivation of the catalyst strongly depended on reaction temperatures. At high reaction temperatures above 300°C, the catalyst did not lose its activity, regardless of SO_2 feed concentration from 500 to 20 000 ppm. However, at low reaction temperatures near 250°C, an apparent deactivation occurred [7,8].

*Corresponding author at address a. Fax: (82-562) 279-8299; e-mail: isnam@vision.postech.ac.kr

0920-5861/97/$32.00
PII S0920-5861(97)00064-3

The deactivation was primarily due to the blocking and/or filling of catalyst pores by deactivation agents. The deactivation agents deposited on the catalyst surface were considered to be basically ammonium salts, such as $(NH_4)_2SO_4$ and/or NH_4HSO_4, formed by the reaction between SO_2 and NH_3 [9]. A honeycomb-type reactor was developed for the reduction of NO_x from stationary sources as a low pressure drop reactor. The reactor was prepared by washcoating zeolite-type catalysts on cordierite honeycomb support with appropriate binders [8]. The reactor configuration including reaction conditions was optimized for the low pressure drop and the high catalytic activity of the honeycomb reactor.

In this study, the catalytic activity of the catalysts was examined in a pilot plant handling 1000 Nm^3/h of actual flue gas from a sintering plant at a steel mill for the commercialization of the catalytic system developed in the present study. The catalyst life due to the deactivation was mainly examined.

2. Experimental

2.1. Catalyst preparation

The copper ion-exchanged hydrogen mordenite (CuHM) and natural zeolite (CuNZA) catalysts were prepared by ion exchange of hydrogen mordenite from PQ Corp. and natural zeolite, composed of mainly mordenite and clinoptiolite, from the area near to Pohang, respectively, with 1 N aqueous solution of cupric nitrate at 80°C for 24 h. The ion-exchanged zeolites were filtered and washed with distilled water. They were dried at 100°C for 12 h and then calcined at 500°C for 3 h in air atmosphere. The copper content in the catalyst were about 2.5 wt%.

The honeycomb reactors employed in the pilot plant were prepared by washcoating of the CuHM and CuNZA with silica binder on the cordierite honeycomb with dimension of 150 × 150 × 100 mm. The washcoated honeycomb was blown with compressed air to remove excess slurry on the honeycomb and then dried at 100°C for 3 h. The amount of catalyst washcoated on the surface of the honeycomb varying 10 to 15% based upon the weight of the honeycomb can be controlled by repeating these procedures. The washcoated honeycomb was calcined at 500°C for 3 h in air.

2.2. Pilot plant description

The flue gas was introduced into the pilot plant at about 130°C by a blower from the side stream of the main duct of the sintering plant of steel mill as shown in Fig. 1. The flue gas, which is produced from the

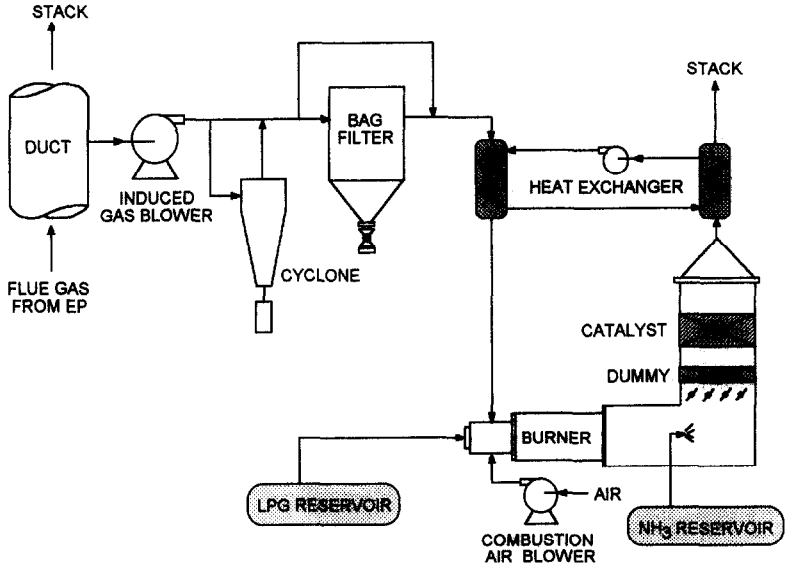

Fig. 1. A schematic flow diagram of the deNO_x pilot plant.

sintering process of iron ore, normally contains NO_x of 200 ppm, SO_x of 200 ppm, CO of 1%, H_2O of about 10% and particulate of about 50 mg/Nm^3. The particulate can be further reduced by a bag filter or a cyclone installed before a heat exchanger. The gas stream which was preheated to about 230°C by the heat effluent heat exchanger was directly heated to the desired reaction temperature by an in situ LPG burner.

The pilot plant was normally operated in the range of 300–700 Nm^3/h and 250–450°C. The NH_3 required for the NO removal was supplied by an NH_3 cylinder. For the complete mixing of NH_3 with the flue gas, an injection nozzle, a baffle of the reactor and a dummy honeycomb layer were installed before the catalytic reactor. The quantity of necessary NH_3 was determined on the basis of the NO_x concentration at the inlet of the reactor. The ratio of NH_3 to NO_x was normally about 1. The NH_3 slip could be controlled to less than 10 ppm by the change of NH_3/NO_x feed ratio. The concentration of NO_x was measured by the on-line chemiluminescence-type NO_x analyzer. All operating parameters of the reaction system were controlled by a computer-interfaced automatic system.

The SCR reactor consists of a dummy honeycomb support layer and a catalytic reactor layer with dimension of 600 × 600 × 100 mm, respectively. The maximum number of catalytic reactor layers which can be installed in the present reactor is four.

3. Results and discussion

3.1. Catalytic activity of CuHM and CuNZA catalysts

Fig. 2 shows the catalytic activity of the CuHM catalyst washcoated on honeycomb-100 cell (CuHM/100-cell) at a space velocity of 10 000 h^{-1} and 400°C. The space velocity was defined as the ratio of the flow rate of the flue gas to the volume of the honeycomb reactor. The experiment was carried out with a bag filter, which can reduce the content of the particulate contained in the flue gas down to about 30 mg/Nm^3. Initial NO conversion of about 93% was decreased to about 85% after 350 h of time-on-stream and maintained up to 460 h with a slight decrease of the activity. When the reaction was carried out without bag filter, NO conversion was decreased up to about 78% within 180 h due to the plugging of the channels of the honeycomb reactor by the particulates included in the flue gas.

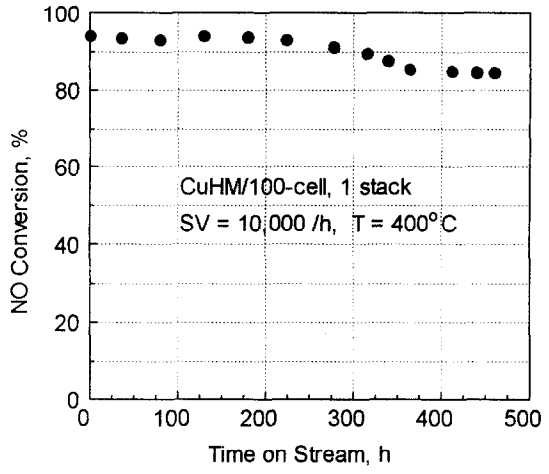

Fig. 2. Catalytic activity of the CuHM/100-cell at the reactor space velocity of 10 000 h^{-1} and 400°C.

The CuNZA catalyst washcoated on the honeycomb-20 cell (CuNZA/20-cell) was employed for its application in the high dust system. The large cell size may improve the deactivation by the plugging of the honeycomb reactor channels due to the particulate. The result of the life test of the CuNZA/20-cell is shown in Fig. 3. The activity was decreased at the initial stage of reaction and leveled off after about 100 h of time-on-stream. The activity of CuNZA/20-cell is lower than that of CuHM/100-cell because of the low surface area of the honeycomb-20 cell and the high space velocity of the reactor. However, the plugging of the honeycomb reactor was significantly improved.

3.2. Catalytic activity in the high dust condition

Fig. 4 shows the result of the life test of the CuNZA/20-cell under high dust conditions operated without a bag filter. During the period of the test, the concentration of the particulate in the flue gas occasionally exceeded 100 mg/Nm^3. The catalytic activity of the CuNZA/20-cell was continuously decreased and was not leveled off. When a cyclone was employed after about 500 h of time-on-stream, the

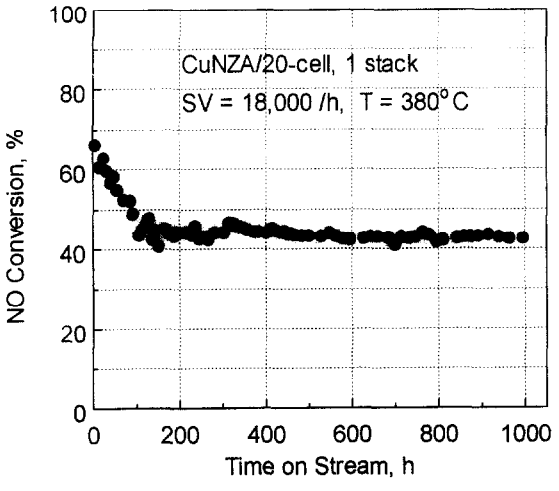

Fig. 3. Catalytic activity of the CuNZA/20-cell at the reactor space velocity of 18 000 h^{-1} and 380°C.

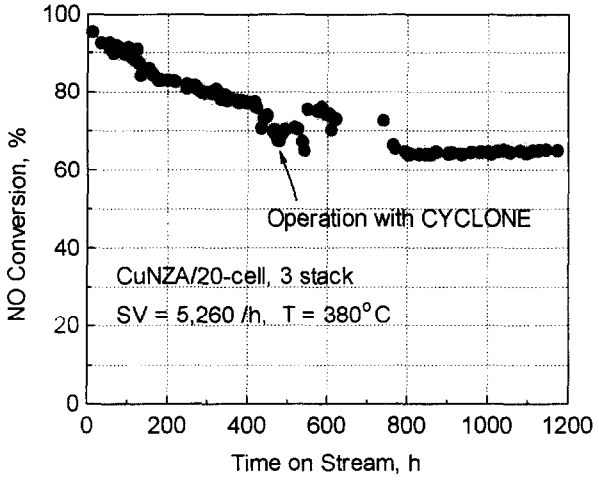

Fig. 4. Catalytic activity of CuNZA/20-cell under high dust conditions operated without a bag filter.

activity was leveled off after about 800 h of time-on-stream. A bag filter or a cyclone, therefore, should be employed to improve the deactivation of the catalyst by the particulate for the high dust operating condition. It can occasionally occur during the periods of shut-down and restart of the sintering plant.

Fig. 5 shows the activity of the CuHM/20-cell operated with the cyclone. The activity was slightly decreased at the initial stage of reaction and remained

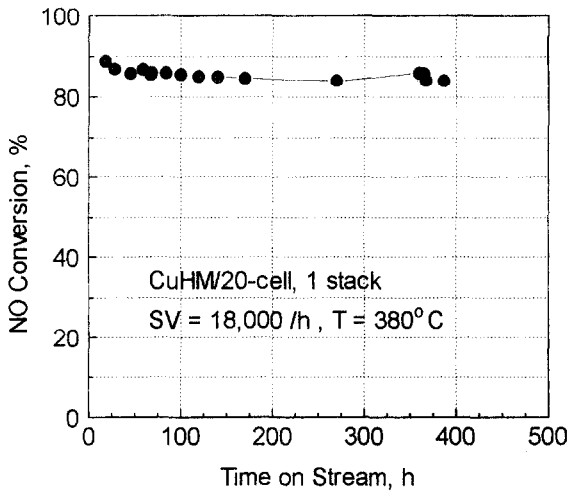

Fig. 5. Catalytic activity of the CuHM/20-cell operated with cyclone.

nearly constant. Compared with the results of Figs. 3 and 5, the activity of CuHM/20-cell was higher than that of CuNZA/20-cell. The result in the laboratory, however, exhibited a similar activity. It seems that the CuHM catalyst is more resistant to deactivation by particulates than the CuNZA catalyst. However, the loss of NO removal activity for CuNZA catalyst can be compensated by the design strategy of the deactivating reactor, such as the overdesign of the reactor, since the activity levels off.

3.3. *Deactivation of the catalyst*

The samples of the CuHM/100-cell catalyst, CuNZA/20-cell catalyst and dummy honeycomb reactor employed in the pilot plant were taken out from the reactor for a better understanding of the cause of the catalyst deactivation. The surface analysis of the deactivated catalyst from the pilot plant was made in the laboratory.

Elementary analysis by the electron-dispersive X-ray spectroscopy (EDS) showed that the particulate deposited on the honeycomb was mainly potassium, sulfur, copper and iron compounds. The deposition of the particulate mostly occurred on the dummy layer and the inlet part of the honeycomb catalyst. Therefore, the installation of the dummy honeycomb layer is very useful to protect the catalytic reactor from the deposition of any deactivating agent.

Fig. 6. Electron probe microanalysis (EPMA) of the CuHM/100-cell used in the pilot plant for 460 h. (mag.: × 1 000) (A) SEM image, (B) S, (C) Cu, (D) K, (E) Fe.

The surface analysis by electron probe microanalysis (EPMA) for the CuHM/100-cell used in the pilot plant has been made as shown in Fig. 6. The map of images represents the distribution of chemical components on the catalyst surface. Potassium, copper and sulfur are predominant species deposited on the catalyst surface. The CuNZA/20-cell also showed similar results. It strongly suggests that the deactivation precursors on the catalyst surface may be related to potassium, copper and sulfur but not to iron.

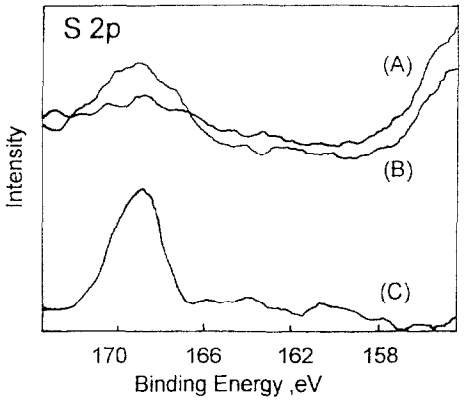

Fig. 7. S 2p X-ray photoelectron spectra of the CuHM/100-cell (A) and dummy honeycomb (B) used in the pilot plant for 460 h and the particulate collected (C).

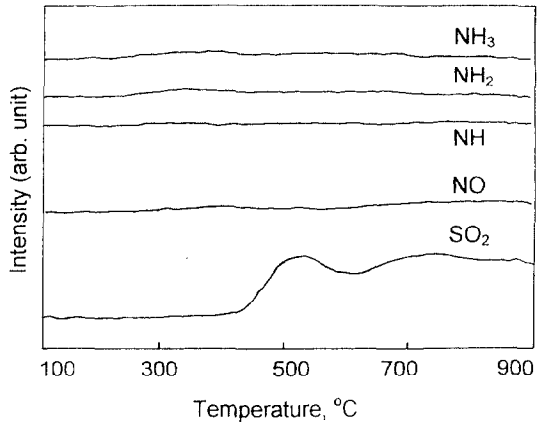

Fig. 8. TPD spectra of the CuHM/100-cell used in the pilot plant for 460 h.

X-ray photoelectron spectroscopy (XPS) analysis was conducted to investigate the state of sulfur deposited on the catalyst surface. The binding energy for S 2p of the deactivated catalysts was about 169.0 eV, indicating that sulfur is present in the form of sulfate [10], as shown in Fig. 7. From the temperature programmed desorption (TPD) experiments of the deactivated catalysts with mass spectrometer as shown in Fig. 8, the formation of ammonium sulfate was not observed. No NH_3 was observed during the desorption experiment, but SO_2 was evidently detected. From the results of EPMA, XPS and TPD experiments, therefore, it was concluded that the deactivation of catalysts was primarily due to the accumulation of sulfate on the catalyst surface by the oxidation of SO_2 in the flue gas to SO_3 on the catalyst surface including metals such as K and Cu. It is believed that the accumulation of sulfate leads to the blocking and filling of the catalyst pores and the decrease of the acidity of the catalyst.

4. Conclusions

The copper-ion-exchanged hydrogen mordenite and natural zeolite catalysts were examined in a pilot plant employing actual flue gas from a sintering plant at a steel mill. The catalysts washcoated on the honeycomb reactor revealed strong tolerances of sulfur and particulates included in the flue gas as well as NO_x. The large cell size of the honeycomb reactor improved deactivation due to the plugging of the channels of the honeycomb reactor by the particulates in the flue gas. The deactivation of catalysts was primarily attributed to the accumulation of sulfate on the catalyst surface. The copper-ion-exchanged zeolite catalyst seems to be a promising catalyst for the SCR of NO_x by NH_3.

References

[1] H. Bosch and F. Jassen, Catal. Today, 2 (1988) 369.
[2] T. Seiyama, T. Arakawa, T. Matsuda, N. Yamazoe and Y. Takita, Chem. Lett., (1975) 781.
[3] I.-S. Nam, J.W. Eldridge and J.R. Kittrell, Stud. Surf. Sci. Catal., 38 (1988) 589.
[4] I.-S. Nam, S.W. Ham, U.C. Hwang and Y.G. Kim, Catal. Sci. Tech., 1 (1991) 165.
[5] I.-S. Nam, S.W. Ham, H. Choi and Y.G. Kim, Stud. Surf. Sci. Catal., 68 (1991) 573.
[6] I.-S. Nam, J.W. Eldridge and J.R. Kittrell, I&EC Prod Res. Dev., 25 (1986) 192.
[7] S.W. Ham, H. Choi, I.-S. Nam and Y.G. Kim, Catal. Today, 11 (1992) 611.
[8] H. Choi, S.W. Ham, I.-S. Nam and Y.G. Kim, I&EC Prod. Res. Dev., 35 (1996) 106.
[9] S.W. Ham, H. Choi, I.-S. Nam and Y.G. Kim, I&EC Prod. Res. Dev., 34 (1995) 1616.
[10] G.E. Mullenberg (Ed.), Handbook of X-ray Photoelectron Spectroscopy, Perkin-Elmer, New York, NY, 1978.